Feature-Based Camera Model Identification Works in Practice
Results of a Comprehensive Evaluation Study

Thomas Gloe, Karsten Borowka, and Antje Winkler

Technische Universität Dresden
Institute of Systems Architecture
01062 Dresden, Germany
{Thomas.Gloe,Antje.Winkler}@tu-dresden.de

Abstract. Feature-based camera model identification plays an important role in the toolbox for image source identification. It enables the forensic investigator to discover the probable source model employed to acquire an image under investigation. However, little is known about the performance on large sets of cameras that include multiple devices of the same model. Following the process of a forensic investigation, this paper tackles important questions for the application of feature-based camera model identification in real world scenarios. More than 9,000 images were acquired under controlled conditions using 44 digital cameras of 12 different models. This forms the basis for an in-depth analysis of a) intra-camera model similarity, b) the number of required devices and images for training the identification method, and c) the influence of camera settings. All experiments in this paper suggest: feature-based camera model identification works in practice and provides reliable results even if only one device for each camera model under investigation is available to the forensic investigator.

1 Introduction

Progress in digital imaging technologies over the past decade enable the acquisition and processing of images in high quality. Consequently, digital images are employed in various settings, ranging from simple snap-shots to professional pictures. Revealing information about the image acquisition device, digital images can form valuable pieces of evidence in forensic investigations to link persons with access to devices of the employed model or with access to the employed device itself.

To identify the source of an image, several approaches have been proposed. They can be broadly separated into four subclasses with increasing granularity: The first class of methods enables a separation between natural and computer generated images [1,2]. Methods to identify the class of the employed image acquisition devices [3], e.g. digital camera, flatbed scanner or camcorder, form the second class. The third class consists of methods to identify the employed device

S. Katzenbeisser and A.-R. Sadeghi (Eds.): IH 2009, LNCS 5806, pp. 262–276, 2009.

model [4,5,6,7,8] and, finally, the fourth class of methods enables to identify the employed source device itself [9,10,11,12,13,14].

This paper belongs to the third class and focuses on feature-based camera model identification, an approach to identify the employed camera model by analysing different model-dependent characteristics. It is based on an approach that has been originally proposed by Kharrazi, Sencar and Memon [4] for digital camera model identification, and has further been investigated by Çeliktutan, Avcibas and Sankur for low resolution cell-phone cameras [6,15]. Using small sets of digital cameras or cell-phone cameras, reliable results for both camera and cell-phone model identification were reported. However, little is known about the real world performance of feature-based camera model identification within forensic investigations, where the number of cameras and models is much larger. In particular, it remains unclear if the features actually capture model-specific characteristics (as claimed in the literature), or rather device-specific components. Recent results by Filler, Fridrich and Goljan [8] strengthened the conjecture that in fact device-specific PRNU might influence the features and thus drive the classification success in Kharrizi et al.'s seminal publication [4].

This study employs a set of 12 digital camera models with altogether 44 digital cameras to analyse the performance of feature-based camera model identification in a realistic forensic investigation scenario. Generally, the features used for camera model identification should be chosen in a way that the intra-camera model similarity is high, i.e., the feature values of devices of the same model are similar. In contrast, the inter-camera model similarity between different camera models should be small.

With respect to the limited resources and limited budget of forensic investigators, this paper contains valuable information regarding the intra-camera model similarity as well as the number of required images and devices for training the identification method by analysing a large camera set. Another important aspect for camera model identification is the influence of typical camera settings, namely, focal length and flash, as well as the influence of scene content. This aspect is investigated by using images acquired with different camera settings.

The remainder of the paper is organised as follows: Section 2 introduces and extends the scheme for camera model identification. Section 3 discusses the employed test setup as well as properties of the acquired images. Section 4 presents and discusses the results for feature-based camera model identification using a large set of camera models and, finally, the paper concludes with a discussion in Section 5.

2 Camera Model Identification

Motivated by differences in the internal image acquisition pipeline of digital camera models, Kharrazi, Sencar and Memon proposed a set of 34 features in order to identify the camera model [4]. They argued that the features were stable for all devices of one model and, therefore, would capture characteristics inherent in each image acquired with the same camera model. The analysed characteristics

can be classified into three main groups: colour features describing the colour reproduction of a camera model, wavelet statistics quantifying sensor noise and image quality metrics measuring sharpness (quality of scene reproduction by the optical system) and noise. Figure 1 illustrates the basis of the three groups in the simplified model of a digital camera.

To create visually pleasing images, the manufacturers specifically fine-tune the used components and algorithms for each digital camera model. Details on this fine-tuning are usually considered as trade secrets. Colour features try to characterise the employed camera model-dependent combination of colour filter array and colour interpolation algorithm as well as the algorithms used in the internal signal-processing pipeline including, for example, its white-point correction.

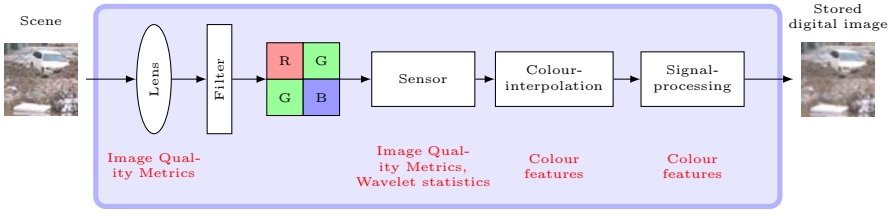

Fig. 1. Simplified image acquisition pipeline of a digital camera model and the main feature groups coarsely capturing characteristics of camera components

Considering the original feature set, Kharrazi et al. propose to use only average values of the three colour channels without analysing their relationships. However, it is important to include the dependencies between the average values of the colour channels. Therefore, 6 additional features characterising white point correction are included. Namely, the factors for white point correction and the difference between the original version and the white-point corrected version of an image measured by the normalised L_1- and L_2-norm are included in the extended set of colour features (see App. A).

Furthermore, we follow Farid and Lyu [16] and Çeliktutan et al. [15] in extending the original set of wavelet statistics by using the empirical standard deviation and skewness of the 3 wavelet sub-bands of the greyscale version of an image. Altogether, the extended feature set consists of 46 different features.

Practical investigations in this paper were done by both using the original feature set proposed by Kharrazi et al. and the extended feature set. Depending on the experiment, the overall success rates could be improved slightly by up to 3 percentage points. For brevity, only the increased performance using the extended feature set is reported here.

To determine the employed source camera model of an image under investigation, a machine-learning algorithm – for example a support vector machine (SVM) [17] – is trained with features of images of each digital camera model

under investigation. Afterwards the trained machine-learning algorithm is ready to determine the corresponding camera model of an image under investigation by finding the closest match of feature values.

3 Practical Test Setup

To study the performance of feature-based camera model identification in a real world scenario, we use a subset of the 'Dresden' image database for benchmarking digital image forensics [18]. Table 1 summarises the 12 selected digital camera models[1], the number of corresponding devices and images, and basic camera specifications. The database includes both, typical consumer digital camera models and digital SLR semi-professional cameras.

Table 1. List of digital cameras in this study, including basic camera specifications. Note, in case of the Nikon D200 digital camera, two SLR-camera bodies were used with interchanging 2 different lenses for each acquired scene.

Camera Model	No. Devices	Resolution [Pixel]	Sensor Size [inch]	Focal Length [mm]	No. of Images (flash off/on)
Canon Ixus 55	1	2592×1944	1/2.5"	5.8−17.4	302 (235/67)
Canon Ixus 70	3	3072×2304	1/2.5"	5.8−17.4	581 (459/122)
Casio EX-Z150	5	3264×2448	1/2.5"	4.65−18.6	941 (761/180)
Kodak M1063	5	3664×2748	1/2.33"	5.7−17.1	1077 (746/331)
Nikon Coolpix S710	5	4352×3264	1/1.72"	6.0−21.6	931 (758/173)
Nikon D200 Lens A/B	2	3872×2592	23.6×15.8 mm	17−55/ 18−135	875 (793/82)
Nikon D70/D70s	2/2	3008×2000	23.7×15.6 mm	18−200	767 (689/78)
Olympus μ1050SW	5	3648×2736	1/2.33"	6.7−20.1	1050 (702/348)
Praktica DCZ 5.9	5	2560×1920	1/2.5"	5.4−16.2	1024 (749/275)
Rollei RCP-7325XS	3	3072×2304	1/2.5"	5.8−17.4	597 (444/153)
Samsung L74wide	3	3072×2304	1/2.5"	4.7−16.7	690 (544/146)
Samsung NV15	3	3648×2736	1/1.8"	7.3−21.9	652 (542/110)
$\sum$	44				9487 (7422/2065)

The employed image database includes 12 camera models with 1 up to 5 available devices for each model. This is substantial more in comparison to existing work, where feature-based camera model identification was tested using a small set of digital cameras (5 camera models) [4] or a small set of cell-phone cameras with low resolution (13 cell-phone models with altogether 16 devices) [15]. Another difference to existing work is the variation of camera settings.

The image database was created using different scenes of natural and urban environments as well as indoor and outdoor environments. To investigate the influence of image content on feature-based camera model identification, a tripod was used to acquire the same scene with each digital camera. The images were acquired using full automatic or, when available, program mode. All images were

[1] Due to the availability of only one single device of camera model Canon Ixus 55, it was not included in all experiments.

stored in the compressed JPEG image file format using the maximum available quality setting and the maximum available resolution. Furthermore, each scene was photographed with each digital camera using 3 different settings of focal length. The flash mode was set to automatic mode and in case of flash release, an additional image was taken with flash turned off. A more detailed description of the 'Dresden' image database has been submitted to another venue [18].

To evaluate the quality of the image database, the number of saturated image pixels was calculated in a greyscale version of each image. Image pixels are counted as saturated if either their value is ≤ 5 or ≥ 250. In brief, 97% of all images contain less than 25% saturated image regions and 89% of all images contain less than 10% saturated image pixels.

All investigations in this paper make use of the support vector machine developed by Chang and Lin with a radial based kernel function [17].

4 Experiments

4.1 Intra- and Inter-Camera Model Similarity

The ability to separate between different camera models and not between different devices is important for all camera model identification schemes. Therefore, the features used for camera model identification should be chosen in a way that the intra-camera model similarity is high, i.e., the feature values of cameras of the same model are similar. In contrast, the inter-camera model similarity between different camera models should be minimised.

To investigate intra-camera model similarity, the feature-based camera model identification scheme is applied in order to identify the employed device (and not the employed camera model – contrary to its original purpose). The intra-camera model similarity is investigated for each camera model independently by training a support vector machine for each device of one model.

Additionally, the similarity between devices of the same series is exemplarily investigated on the basis of the Canon Ixus 55 and the Canon Ixus 70 cameras, which are equipped with similar optics and equally sized sensors but provide different sensor resolutions. Generally it is expected that devices of the same series are difficult to separate.

The support vector machine is trained with 60% of the images of each device for training and the remaining images are used for testing. The test is repeated 250 times for each camera model, and within each run, the images are randomly assigned to either the training or test set.

Table 2 summarises the results for image source identification in case of devices of the series Canon Ixus. This test illustrates two important aspects: First, images acquired with devices of the same series are correctly assigned to the corresponding camera model with an negligible false identification rate, and, second, images acquired with devices of the same model are assigned diffusely within the corresponding set.

Table 2. Intra-camera similarity in case of the camera model series Canon Ixus (overall correct device identification 79.67%)

	Identified as			
Device	Ixus 55	Ixus 70 A	Ixus 70 B	Ixus 70 C
Ixus 55	**99.99**	-	0.01	-
Ixus 70 A	-	**74.50**	11.92	13.57
Ixus 70 B	0.06	16.49	**68.03**	15.43
Ixus 70 C	0.08	18.77	16.42	**64.72**

Reconsidering the aspect of diffuse assignment of images within the corresponding set of devices of the same model, the results summarised in Tab. 3 support this observation for camera model Casio EX-Z150 and illustrate another interesting effect: Device B of the Casio EX-Z150 model represents a centroid in the feature space of all devices of this model. Consequently, the probability of assigning images to device B is higher than for all other devices of the Casio EX-Z150. In contrast to the results for Canon Ixus 70, the images are assigned more diffusely, which indicates a better intra-camera model similarity.

Table 3. Intra-camera similarity in case of camera model Casio EX-Z150 (overall correct device identification 18.64%)

	Identified as				
Device	Casio A	Casio B	Casio C	Casio D	Casio E
Casio A	13.96	**39.54**	22.69	13.98	9.83
Casio B	17.55	**34.46**	24.06	12.94	10.99
Casio C	14.77	**37.64**	22.23	14.10	11.26
Casio D	15.23	**36.23**	23.03	12.57	12.94
Casio E	13.44	**37.22**	22.41	17.15	9.78

Within the employed image database, the results for the Nikon D200 represent an anomaly. In contrast to the results for all other camera models, Tab. 4 illustrates that correct device identification is possible with a correct identification rate of 98.41% using the feature-based camera model identification scheme. This result is unexpected, especially due to the fact that both devices acquired images of each scene by interchanging the employed lenses. Possibly, the intra-camera model deviation within this class of semi-professional SLR cameras is larger than in case of typical consumer cameras, which leads to the clear separability. Future research has to include more devices of the same semi-professional SLR camera model to further investigate this aspect.

To visualise intra-camera model similarity as well as inter-camera dissimilarity of all employed devices, the 10 most influential features for separating all devices are selected using principal component analysis and the calculated centroids are mapped to a 2D-plot depicted in Fig. 2. The calculated plot supports the

Table 4. Intra-camera similarity in case of camera model Nikon D200 SLR (overall correct device identification 98.41%)

Device	Identified as Nikon D200 A	Nikon D200 B
Nikon D200 A	**98.73**	1.27
Nikon D200 B	1.97	**98.03**

discussed aspects of intra-camera model similarity and clearly visualises inter-camera model dissimilarity as a basis for differentiating between camera models. For example, the calculated centroids of the 5 Casio EX-Z150 cameras are very close to each other. This is similar for all other camera models except the Nikon D200 SLR. Moreover, the deviation between centroids of the Samsung NV15 devices is larger than for other camera models.

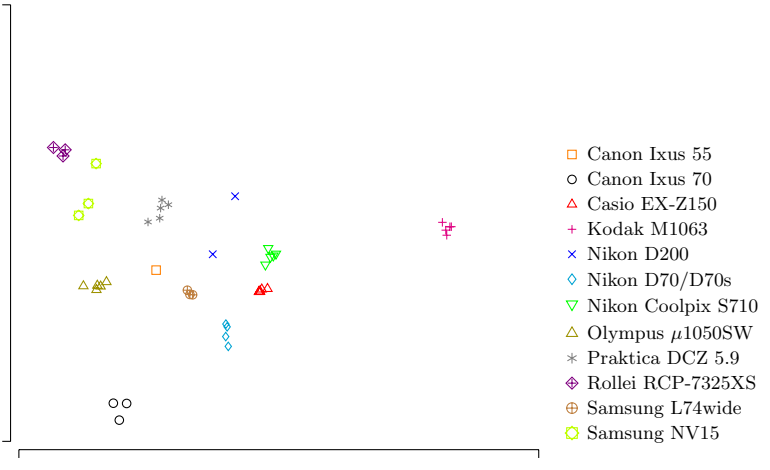

Fig. 2. Calculated 10 most influential features to characterise each device plotted to 2D using multidimensional scaling. Each symbol of one camera model corresponds to the centroid of one device. The centroids of devices of the same model are close to each other whereas the centroids of other models are farther apart.

Figure 2 visualises only the centroid of each device of one model in a 2D mapping of the feature subspace. To illustrate the separability between images of different camera models, Fig. 3 depicts a 2D plot of the calculated features of all images in the database for the camera model Canon Ixus 70 and the camera model Nikon Coolpix S710 using multidimensional scaling. As expected, it is possible to clearly separate between both camera models but not between different devices of one model. Thus, the features are appropriate for camera model identification.

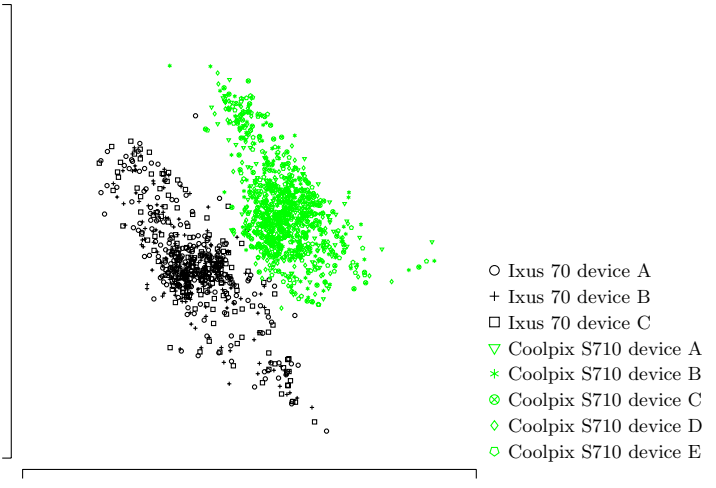

Fig. 3. 2D plot of the two most distinctive principal components of the calculated features of all images acquired with the model Canon Ixus 70 (black) and of all images acquired with the model Nikon Coolpix S710 (green). Inter-camera model variation is larger than intra-camera model variation, hence, a clear separation between images acquired with the Ixus 70 and the S710 is possible. Different symbols of the same colour indicate the device of each model, hence, a separation between devices of the same model is not possible.

4.2 Naive Test of Feature-Based Camera Model Identification

A first naive test of feature-based camera model identification on the image database investigates the reliability of the method. Therefore, we select for each model 60% of the devices and used all corresponding images for training. The images of the remaining devices are used for testing the identification algorithm. In case of the Nikon D200 SLR camera model, one device is assigned for training and the other device is assigned for testing the performance of the identification method.

This approach simulates a typical forensic investigation scenario, where several camera models in question are purchased and used for training the identification scheme and the images under investigation correspond to the test set. To measure the influence of the number of selected devices for the training and the test set, the naive test scenario is repeated 15 times while the assignment of each device either to the training or to the test set is iterated over all possible combinations.

Table 5 summarises the results for correct camera model identification. In all cases, the majority of test images is correctly assigned to the correct camera model. The achieved results are convincing and promise a correct camera model identification for more than 98% of all images of all camera models with exception of the Nikon D200. The results for the Nikon D200 are similar to the investigations of the intra-camera model similarity. Compared to other camera

models in the image database, the employed devices of this model are more dissimilar and a larger number of devices would be required for training.

The fact that the image database includes images of varying focal length, different environments and different flash settings implies that no special support vector machines have to be trained for each camera setting. These are very good news with regard to the required effort of a forensic image investigation.

Table 5. Results for camera model identification: 60% of the devices of each model are selected and the corresponding images are used for training. Images of the remaining devices are used for testing (overall correct model identification performance 97.79%, worst result 96.5% and best result 98.7%).

	Identified as									
Camera model	I	E	M	DT	DS	μ	DC	R	L	N
Ixus 70 (I)	**99.28**	-	-	-	0.07	0.14	-	-	0.52	-
EX-Z150 (E)	0.02	**99.95**	-	-	0.02	-	-	0.02	-	-
M1063 (M)	-	-	**99.97**	-	-	-	-	-	-	0.03
D200 (DT)	1.89	1.65	1.00	**88.31**	-	5.51	-	0.55	0.03	1.06
D70/D70s (DS)	0.58	0.31	0.14	0.10	**97.94**	0.02	0.12	-	0.71	0.07
μ1050SW (μ)	0.46	0.32	-	0.24	-	**98.48**	0.03	0.02	0.03	0.43
DCZ 5.9 (DC)	-	-	-	-	0.62	-	**99.36**	0.02	-	-
RCP-7325XS (R)	-	-	-	-	-	-	-	**100.00**	-	-
L74Wide (L)	0.14	-	-	-	0.03	-	-	-	**99.83**	-
NV15 (N)	0.03	-	0.61	0.03	0.03	0.37	-	-	-	**98.93**

However, the applied naive test includes two weak points: First, images in the image database for each device were acquired using the same scene, which is very unlikely for a forensic investigation, and, second, the size of the images is different for each model, which might 'leak' information about the employed camera model.

4.3 Critical Test of Feature-Based Camera Model Identification

To form a more critical test of feature-based camera model identification, the influence of the number of devices and images available for training is investigated. In contrast to the naive test, images with similar scene content are either included in the training or in the test set of images. Furthermore the overall number of images used for training and testing is fixed to 175 per device, which equals to the minimum number of available images for each device.

Similar to the naive test, the influence of the selected devices is measured by repeating the tests 15 times. The assignment of a device to the training and test set is iterated over all possible variations. The tests are repeated with 10% (17 images), 20% (35 images), 30% (52 images), 40 % (70 images), 50% (87 images), 60% (105 images), 70% (122 images), 80% (140 images) and 90% (157 images) of the fixed set of 175 images per device for training and the remaining images with dissimilar scene content for testing.

Depending on the available number of devices for each camera model, the number of employed devices is varied between 1 up to 4 devices for training. Camera models with less than 5 devices are used with the maximum available number of cameras for training, whereas always one device is include in the test set only. This scenario seems to be similar to a real forensic investigation, where it might be impossible to purchase the same number of devices for each model.

Table 6 and 7 exemplarily summarise the results for varying the number of images employed for training the machine-learning algorithm. The correct camera model identification performance clearly increases with the number of employed images for training from 74.7% in case of 10% of all images up to 95.65% in case of 90% of all images. The reliable performance in case of using 90% of all images of one device for training is only slightly increased by using more than one device for training the machine-learning algorithm: 96.64% for ≤ 2 devices for training, 97.30% for ≤ 3 devices for training and 96.79% for ≤ 4 devices for training.

Observe that the number of camera models employed for training the support vector machine is negligible compared to the number of required images to train the classification algorithm reliable. Furthermore, the results are similar to the naive test indicating that the feature set is quite invariant to scene content. So during a forensic investigation of digital images, it is not necessary to acquire images with the same scene content like the images under investigation and it also seems unnecessary to purchase more than one device for each model.

To tackle the second weak point of the naive test – the possible influence of image size on the feature-based camera model identification scheme – all images are cropped to the same size in the frequency domain without applying recompression. Thus, no new JPEG-compression artefacts distort the test results. The smallest image size in the image database (2560×1920, Praktica DCZ 5.9) is used to crop the images to constant size.

The previous test of this subsection is repeated with the cropped images. Table 8 exemplarily summarises the results for camera model identification using 90% of all cropped images of one device for each camera model for training and the remaining cropped images for testing. Compared to the corresponding test in this subsection that used images in their original size, the overall correct camera model identification performance considerably decreases from 95.65% to 89.66% for the cropped images. Apparently, there is an influence of image size on feature-based camera model identification. A closer look at the results indicates that the performance decrease is different for the camera models and most evident for the camera models Nikon D200, Nikon D70/D70s and Samsung NV15. In practice, this effect might be negligible for images available in their original size. However, in all cases where it is difficult to validate the originality of the image size, it is important to know this effect for correct result interpretation.

Figure 4 summarises the overall results for correct camera model identification varying the number of images and the number of devices used for testing. This visualisation clearly depicts the performance increase depending on the number of employed images for training and the performance decrease between original sized and cropped images. Additionally, the number of devices used for training

Table 6. Results for camera model identification using 10% of the images of 1 device of each model for training and 90% of the images of the remaining devices for testing (overall correct model identification performance 74.70%, worst result 72.42% and best result 79.75%)

	Identified as										
Camera model	I	E	M	DT	DS	S	μ	DC	R	L	N
Ixus 70 (I)	**66.60**	1.53	-	1.34	3.95	-	7.18	0.70	0.25	15.16	3.29
EX-Z150 (E)	1.83	**84.51**	0.32	6.05	3.21	-	0.32	1.91	-	1.86	-
M1063 (M)	-	6.01	**90.63**	1.48	0.25	1.62	-	-	-	-	-
D200 (DT)	6.43	8.62	8.45	**60.40**	0.08	2.46	3.65	2.78	1.21	2.31	3.95
D70/D70s (DS)	6.79	7.52	0.17	1.23	**56.23**	-	0.20	16.52	0.13	11.21	-
S710 (S)	-	0.65	0.12	-	0.01	**96.57**	0.88	-	-	-	1.77
μ1050SW (μ)	9.69	3.29	-	0.96	0.34	-	**54.34**	0.29	0.89	3.73	26.48
DCZ 5.9 (DC)	0.38	1.33	-	0.20	7.42	-	0.73	**86.59**	0.50	2.52	0.33
RCP-7325XS (R)	2.10	0.06	-	0.06	0.79	-	6.14	3.97	**85.43**	0.34	1.10
L74wide (L)	16.56	20.51	-	0.45	3.97	-	2.99	3.57	0.42	**51.52**	-
NV15 (N)	4.54	1.15	-	5.03	0.13	1.30	22.99	4.01	1.49	0.04	**59.32**

Table 7. Results for camera model identification using 90% of the images of 1 device of each model for training and 10% of the images of the remaining devices for testing (overall correct model identification performance 95.65%, worst result 93.40% and best result 97.33%)

	Identified as										
Camera model	I	E	M	DT	DS	S	μ	DC	R	L	N
Ixus 70 (I)	**100.00**	-	-	-	-	-	-	-	-	-	-
EX-Z150 (E)	-	**99.50**	-	0.49	-	-	-	-	-	-	-
M1063 (M)	-	0.39	**97.74**	1.86	-	-	-	-	-	-	-
D200 (DT)	0.39	0.20	0.78	**96.86**	-	-	0.78	-	-	-	0.98
D70/D70s (DS)	2.88	2.09	1.57	0.52	**79.47**	-	-	0.52	-	12.68	0.26
S710 (S)	-	-	-	-	-	**100.00**	-	-	-	-	-
μ1050SW (μ)	1.57	-	-	0.59	-	-	**89.11**	-	-	-	8.73
DCZ 5.9 (DC)	-	-	-	-	1.96	-	-	**98.3**	-	-	-
RCP-7325XS (R)	-	-	-	-	-	-	-	-	**100.00**	-	-
L74wide (L)	0.20	0.98	-	-	0.20	-	-	-	-	**98.62**	-
NV15 (N)	0.59	-	-	0.98	-	-	3.73	-	-	-	**94.70**

the machine-learning algorithm increases the correct identification performance only slightly.

In case of the cropped images an anomaly occurs in the overall performance results. The overall results for camera model identification decrease with the number of employed devices, which is absolutely unexpected. This effect can be traced back to the influence of the Nikon D200 digital SLR camera only. Increasing the number of devices employed for training the machine-learning algorithm obviously complicates the correct separation of the camera model Nikon D200 from other devices. The reason is probably the observed intra-camera model dissimilarity, which emphasises the need for a larger number of devices of this model in the image database.

Table 8. Results for camera model identification using 90% of the cropped images of 1 device of each model for training and 10% of the cropped images of the remaining devices for testing (overall correct model identification performance 89.66%, worst result 85.74% and best result 93.23%)

	Identified as										
Camera model	I	E	M	DT	DS	S	μ	DC	R	L	N
Ixus 70 (I)	**97.64**	-	-	-	-	-	1.37	0.20	-	-	0.78
EX-Z150 (E)	0.49	**93.72**	-	0.29	0.20	1.76	-	0.20	-	3.33	-
M1063 (M)	-	0.49	**98.13**	0.29	1.08	-	-	-	-	-	-
D200 (DT)	8.04	0.78	-	28.43	**40.00**	1.37	-	8.63	-	12.16	0.59
D70/D70s (DS)	1.70	1.70	2.22	10.85	**75.81**	1.70	-	-	-	3.66	2.35
S710 (S)	-	0.20	-	-	-	**99.60**	0.20	-	-	-	-
μ1050SW (μ)	0.10	-	-	-	1.57	-	**94.11**	1.08	-	0.20	2.94
DCZ 5.9 (DC)	-	-	-	0.29	0.10	0.10	0.10	**98.23**	-	-	1.18
RCP-7325XS (R)	-	-	-	0.20	-	-	-	1.57	**98.23**	-	-
L74wide (L)	1.37	0.59	-	0.20	2.55	-	0.20	0.78	-	**94.31**	-
NV15 (N)	8.43	-	-	0.20	-	0.20	2.55	8.24	0.20	0.78	**79.41**

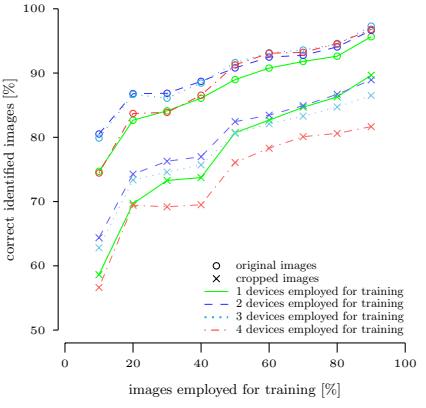

Fig. 4. Overall results for correct camera model identification in relation to maximum number of employed devices and in relation to the employed number of images for training. The remaining images are used for testing the method. Note, the number of images is fixed to 175 images, which equals the smallest number of images available for each camera model.

Figure 5 depicts overall performance results exemplarily for the Casio EX-Z150 camera model and for the Samsung NV15 camera model. Depending on the camera model, the influence of the number of images employed for training and the influence of cropping varies. In case of the Casio EX-Z150, the number of required images to obtain identification results $\geq$ 90% is considerably lower than in case of the Samsung NV15 camera model. This conforms with the calculated intra-camera model similarity of both camera models, which is higher for the Casio EX-Z150 and obviously results in a lower number of required images for training.

Fig. 5. Selected results for correct camera model identification of Casio EX-Z150 and Samsung NV 15 in relation to maximum number of employed devices / number of employed images for training and number of employed images for testing the identification scheme

5 Concluding Remarks

The reported results in this paper document that feature-based camera model identification works in practice. Generally, it enables reliable identification results and therefore is a valuable method in the toolbox for image source identification. The very good news for the limited budget and the limited resources of all forensic investigators is: it is not necessary to buy several devices of one model in order to train the feature-based camera model identification scheme accurately. In fact it is much more important to increase the number of acquired images for training each camera model. It is expected that increasing the number of acquired images in the critical test to a similar level of the naive test increases the results for correct camera model identification. Furthermore, it seems unnecessary to acquire images of scenes with similar content for training the machine-learning algorithm. In fact the dependence between scene content and calculated features appears negligible. Note that the fraction of saturated image pixels was constantly low for all images used for training the machine learning algorithm. It is also important to mention that it is not necessary to train the feature-based camera model identification scheme for each camera setting separately. In fact reliable results are obtained in case of mixed image sets covering different camera settings.

The semi-professional digital SLR camera Nikon D200 turned out to behave anomalous in the employed image database. The intra-camera model similarity of this camera model is very high, thus enabling reliable source camera identification using the feature-based camera model identification scheme. More devices are needed in the training set to tell whether this anomaly is due to a malfunction of one of our test cameras or a more systematic phenomenon. This aspect

will be further investigated in future work using more devices of this camera model and other SLR cameras.

Acknowledgements

The authors would like to thank Rainer Böhme for fruitful discussions and all sponsors for borrowing their camera equipment. Namely, the staff members of the faculty of computer science, the staff members of the AVMZ (TU Dresden), and the following companies for their generous support (in alphabetical order): AgfaPhoto & Plawa, Casio, FujiFilm, Kodak, Nikon, Olympus, Pentax, Praktica, Ricoh, Rollei, Samsung and Sony. Special thanks go to our colleagues and friends supporting the creation of the underlying image database during some of the probably coldest days of the year.

References

1. Lyu, S., Farid, H.: How realistic is photorealistic? IEEE Transactions on Signal Processing 53(2), 845–850 (2005)
2. Dehnie, S., Sencar, H.T., Memon, N.: Digital image forensics for identifying computer generated and digital camera images. In: Proceedings of the 2006 IEEE International Conference on Image Processing (ICIP 2006), pp. 2313–2316 (2006)
3. Khanna, N., Mikkikineni, A.K., Chiu, G.T.C., Allebach, J.P., Delp, E.J.: Forensic classification of imaging sensor types. In: Delp, E.J., Wong, P.W. (eds.) Proceedings of SPIE: Security and Watermarking of Multimedia Content IX, vol. 6505 (2007), 65050U
4. Kharrazi, M., Sencar, H.T., Memon, N.: Blind source camera identification. In: Proceedings of the 2004 IEEE International Conference on Image Processing (ICIP 2004), pp. 709–712 (2004)
5. Bayram, S., Sencar, H.T., Memon, N.: Improvements on source camera-model identification based on CFA. In: Proceedings of the WG 11.9 International Conference on Digital Forensics (2006)
6. Çeliktutan, O., Avcibas, İ., Sankur, B.: Blind identification of cellular phone cameras. In: Delp, E.J., Wong, P.W. (eds.) Proceedings of SPIE: Security and Watermarking of Multimedia Content IX, vol. 6505 (2007), 65051H
7. Swaminathan, A., Wu, M., Liu, K.J.R.: Nonintrusive component forensics of visual sensors using output images. IEEE Transactions on Information Forensics and Security 2(1), 91–106 (2007)
8. Filler, T., Fridrich, J., Goljan, M.: Using sensor pattern noise for camera model identification. In: Proceedings of the 2008 IEEE International Conference on Image Processing (ICIP 2008), pp. 1296–1299 (2008)
9. Lukáš, J., Fridrich, J., Goljan, M.: Determining digital image origin using sensor imperfections. In: Said, A., Apostolopoulus, J.G. (eds.) Proceedings of SPIE: Image and Video Communications and Processing, vol. 5685, pp. 249–260 (2005)
10. Chen, M., Fridrich, J., Goljan, M.: Digital imaging sensor identification (further study). In: Delp, E.J., Wong, P.W. (eds.) Proceedings of SPIE: Security and Watermarking of Multimedia Content IX, vol. 6505 (2007), 65050P

11. Gloe, T., Franz, E., Winkler, A.: Forensics for flatbed scanners. In: Delp, E.J., Wong, P.W. (eds.) Proceedings of SPIE: Security, Steganography, and Watermarking of Multimedia Contents IX, vol. 6505 (2007), 65051I
12. Gou, H., Swaminathan, A., Wu, M.: Robust scanner identification based on noise features. In: Delp, E.J., Wong, P.W. (eds.) Proceedings of SPIE: Security and Watermarking of Multimedia Content IX, vol. 6505 (2007), 65050S
13. Khanna, N., Mikkikineni, A.K., Chiu, G.T.C., Allebach, J.P., Delp, E.J.: Scanner identification using sensor pattern noise. In: Delp, E.J., Wong, P.W. (eds.) Proceedings of SPIE: Security and Watermarking of Multimedia Content IX, vol. 6505 (2007), 65051K
14. Goljan, M., Fridrich, J., Filler, T.: Large scale test of sensor fingerprint camera identification. In: Delp, E.J., Dittmann, J., Memon, N., Wong, P.W. (eds.) Proceedings of SPIE: Media Forensics and Security XI, vol. 7254, 7254–18 (2009)
15. Çeliktutan, O., Sankur, B., Avcibas, İ.: Blind identification of source cell-phone model. IEEE Transactions on Information Forensics and Security 3(3), 553–566 (2008)
16. Farid, H., Lyu, S.: Higher-order wavelet statistics and their application to digital forensics. In: IEEE Workshop on Statistical Analysis in Computer Vision (in conjunction with CVPR) (2003)
17. Chang, C.C., Lin, C.J.: LIBSVM: A library for support vector machines (2001), `http://www.csie.ntu.edu.tw/~cjlin/libsvm`
18. Gloe, T., Böhme, R.: The 'Dresden' image database for benchmarking digital image forensics. Submitted to the 25th Symposium on Applied Computing, ACM SAC 2010 (2010)
19. Adams, J., Parulski, K., Spaulding, K.: Color processing in digital cameras. IEEE Micro. 18(6), 20–30 (1998)

A Additional Colour Features

To get natural-looking images, white-point correction is a very important step in the signal-processing pipeline of a digital camera. The simplest model for white-point correction is based on the grey world assumption [19], where the average of each colour channel is assumed to be equal, or generally speaking a grey value. To apply white-point correction using the grey world assumption, the following equations are applied to the red and blue colour channel:

$$\hat{\mathbf{i}}_{\mathrm{r}} = \frac{\mathrm{avg}(\mathbf{i}_{\mathrm{g}})}{\mathrm{avg}(\mathbf{i}_{\mathrm{r}})} \cdot \mathbf{i}_{\mathrm{r}} \qquad \hat{\mathbf{i}}_{\mathrm{b}} = \frac{\mathrm{avg}(\mathbf{i}_{\mathrm{g}})}{\mathrm{avg}(\mathbf{i}_{\mathrm{b}})} \cdot \mathbf{i}_{\mathrm{b}}, \tag{1}$$

where $\mathrm{avg}(\mathbf{i}_{\mathcal{C}})$ denotes the average of all intensity values in colour channel $\mathcal{C}$ and $\hat{\mathbf{i}}_{\mathcal{C}}$ indicates the white-point corrected version of colour channel $\mathcal{C}$.

The proposed additional colour features are calculated as follows:

$$F_1 = \frac{1}{3}(|\mathrm{avg}(\mathbf{i}_{\mathrm{r}}) - \mathrm{avg}(\mathbf{i}_{\mathrm{g}})| + |\mathrm{avg}(\mathbf{i}_{\mathrm{r}}) - \mathrm{avg}(\mathbf{i}_{\mathrm{b}})| + |\mathrm{avg}(\mathbf{i}_{\mathrm{g}}) - \mathrm{avg}(\mathbf{i}_{\mathrm{b}})|) \tag{2}$$

$$F_2 = \frac{\mathrm{avg}(\mathbf{i}_{\mathrm{g}})}{\mathrm{avg}(\mathbf{i}_{\mathrm{r}})} \quad F_3 = \frac{\mathrm{avg}(\mathbf{i}_{\mathrm{g}})}{\mathrm{avg}(\mathbf{i}_{\mathrm{b}})} \tag{3}$$

$$F_4 = \frac{1}{3} \sum_{\mathcal{C} \in \{\mathrm{r,g,b}\}} ||\mathbf{i}_{\mathcal{C}} - \hat{\mathbf{i}}_{\mathcal{C}}||_{\bar{1}} \tag{4}$$

$$F_5 = ||\mathbf{i}_r - \hat{\mathbf{i}}_r||_{\bar{2}} \quad F_6 = ||\mathbf{i}_b - \hat{\mathbf{i}}_b||_{\bar{2}} \tag{5}$$